Electronic Supplementary Material (ESI) for Catalysis Science & Technology.

Supplementary materials for

Confinement of nano-gold in 3D hierarchically structured gadolinium-doped ceria mesocrystal: synergistic effect of chemical composition and structural hierarchy in CO and propane oxidation.

Piotr Woźniak*[a], Małgorzata A. Małecka[a], Piotr Kraszkiewicz[a], Włodzimierz Miśta[a], Oleksii Bezkrovnyi[a], Lidia Chinchilla[b], Susana Trasobares[b]

[a]Institute of Low Temperature and Structure Research, Polish Academy of Sciences, P.O. Box 1410, 50-950 Wrocław 2, Poland

[b]Departamento de Ciencia de los Materiales e Ing. Metalúrgica y Química Inorgánica, Universidad de Cádiz, Campus Universitario de Puerto Real, 11510, Cádiz - España

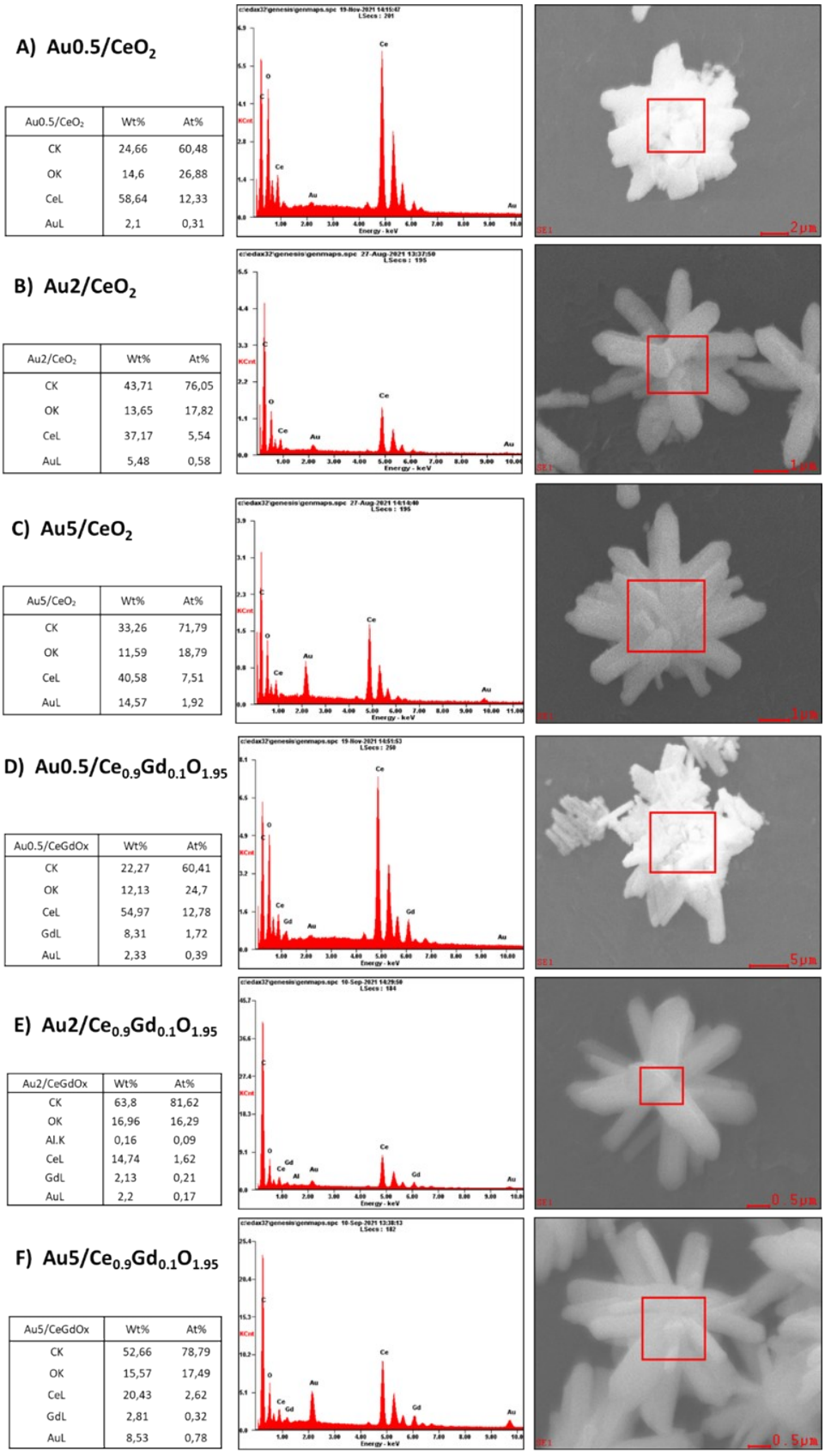

Fig. S1 A-F) SEM-EDX elemental analysis of the hierarchically structured gold-decorated catalysts Au x/$Ce_{1-y}Gd_yO_{2-y/2}$ (x -the surface coverage parameter value ; y= 0 or 0.1). For each material from A to F measurements of 3-5 particles were collected and average at% and wt% values has been calculated; method of calculation and results are shown and described in Fig. 4.D.

A)

Catalyst architecture (gold loading)		
Sample	Au NPs size	
HS NPs (SC nominal)	TEM volume-weighted mean	PXRD
$Au0.5/CeO_2$	-	-
$Au2/CeO_2$	4.8	4.6
$Au5/CeO_2$	4.5	3.9
Au0.5/GDC-10%	-	-
Au2/GDC-10%	4.1	3.6
Au5/GDC-10%	6.7	3.8

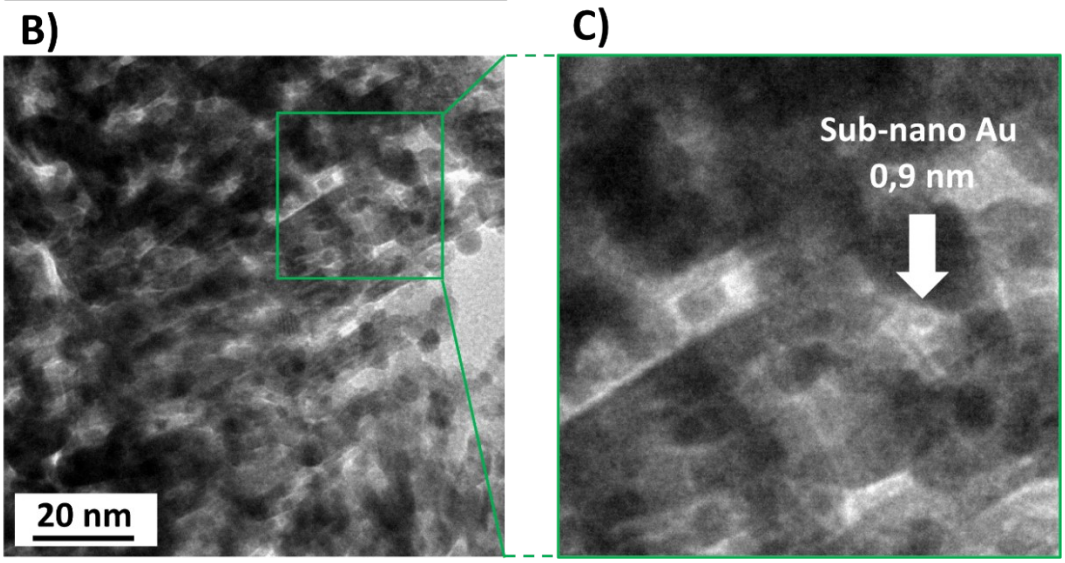

Fig. S2 A) Volume-weighted mean size (obtained from TEM) vs mean size obtained from PXRD (Scherrer formula) of Au NPs on the Au x/HSNPs catalysts differed by gold loading (x indicate SC value = 0.5, 2 or 5) ; B) TEM image of $Au5/CeO_2$ HSNPs sample C) Magnification of the area marked in the image B showing sub-nanometer gold nanoparticle.

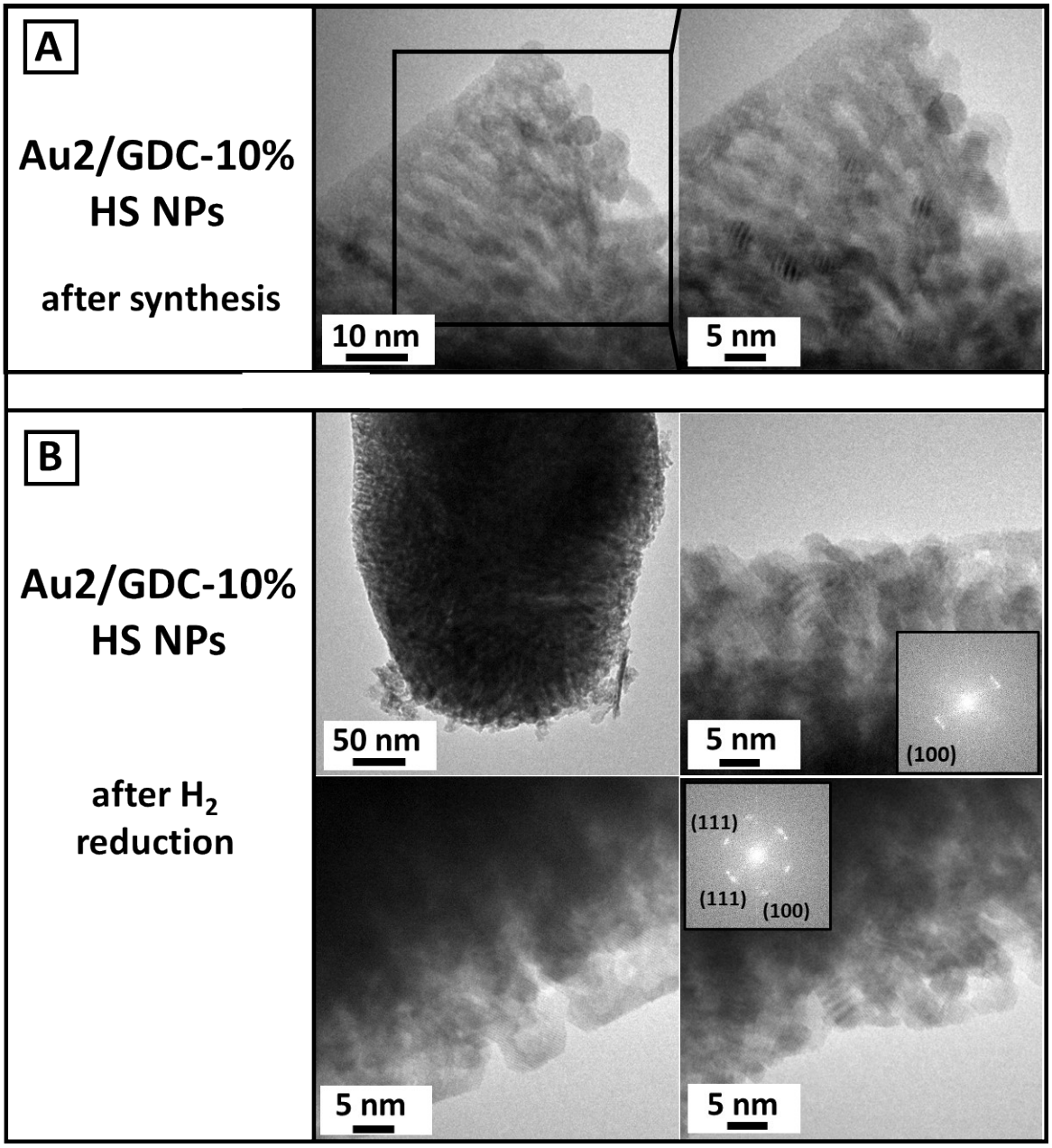

Fig. S3. A) Au2/GDC-10% HSNPs after synthesis. Gold NPs within hierarchical structure visible as Moiré patterns; B) Au2/GDC-10% HS NPs catalyst reduced at 400℃ in H_2 flow for 3h. No Au NPs abundance has been observed on the external surface of the arm of star-shaped hierarchical carrier. Moiré patterns suggest occurrence of Au NPs in the sub-surface regions and inside the hierarchical structure.

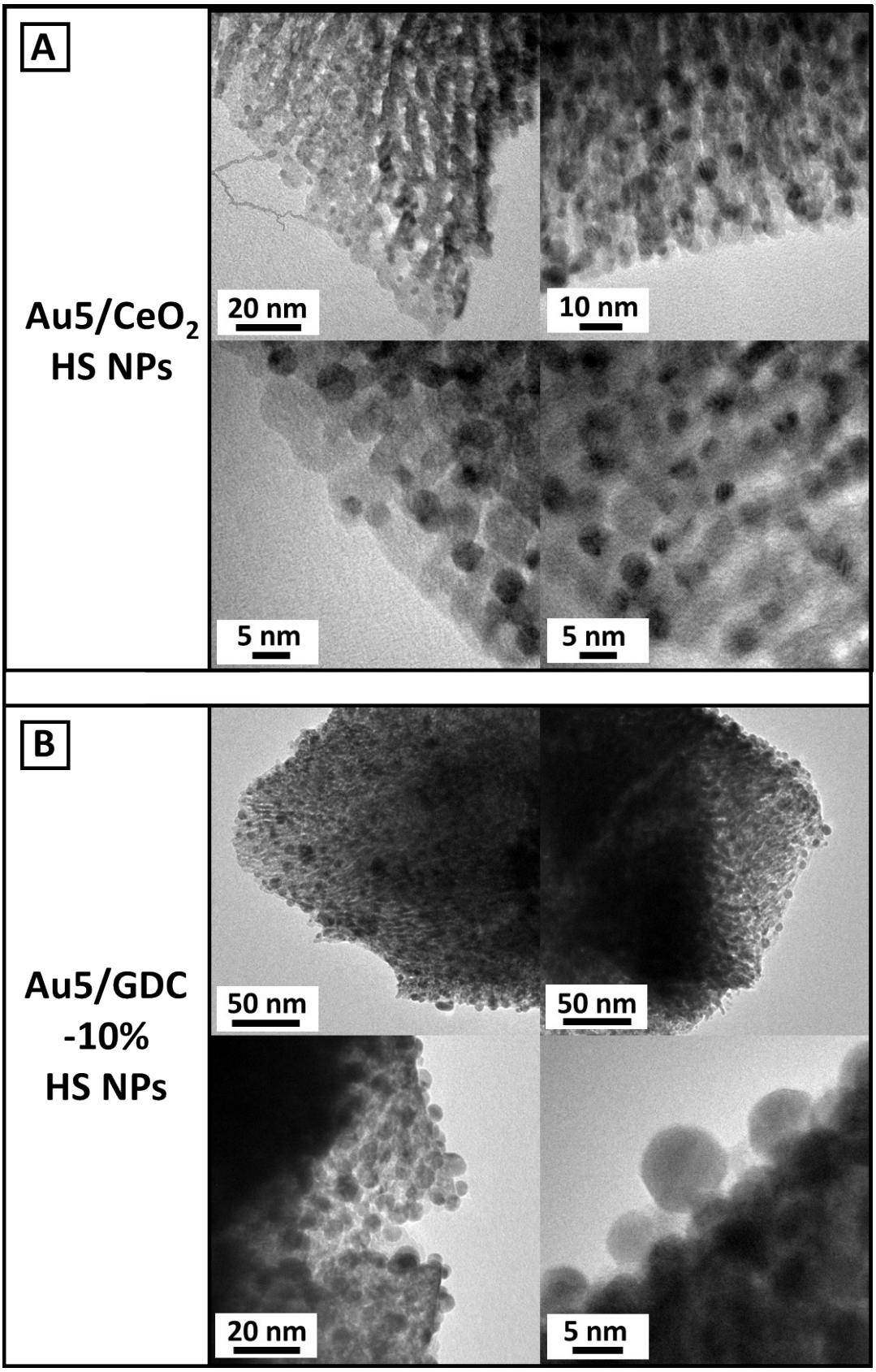

Fig. S4. A) TEM images of gold-decorated Au5/$Ce_{1-x}Gd_xO_{2-x/2}$ (x=0; 0.1) HS NPs catalysts. A) Au5/CeO_2 catalyst; Au NPs observed both, on the external surface of star-shaped ceria carrier and inside the pores in sub-surface (TEM-transparent) region of sample; B). Au5/GDC-10% HS NPs catalysts; Au NPs observed mostly on the external surface of star-shaped particle arms.

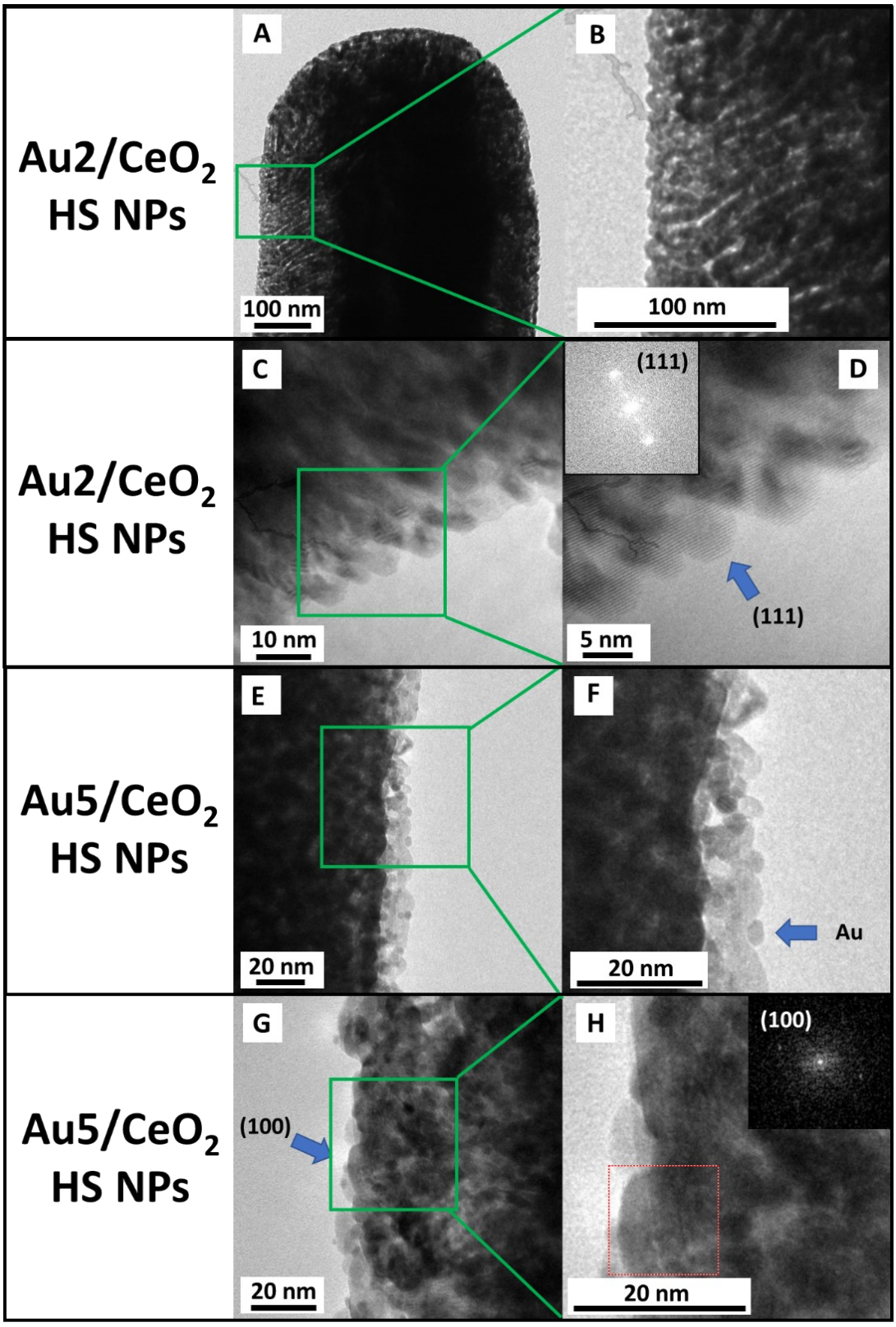

Fig. S5. Morphology of the external surface of the arms of star-shaped Au x/CeO_2 hierarchical catalyst (x denotes surface coverage parameter equal to 2 or 5). A-B) TEM images of Au2/CeO_2 arm showing diversified support surface morphology; C-D) TEM images of Au2/CeO_2 showing exposition of CeO_2(111) planes; E-F) TEM images of Au5/CeO_2 showing Au NPs embedded between CeO_2 crystallites; G-H) TEM images of Au5/CeO_2 showing exposition of CeO_2(100) planes.

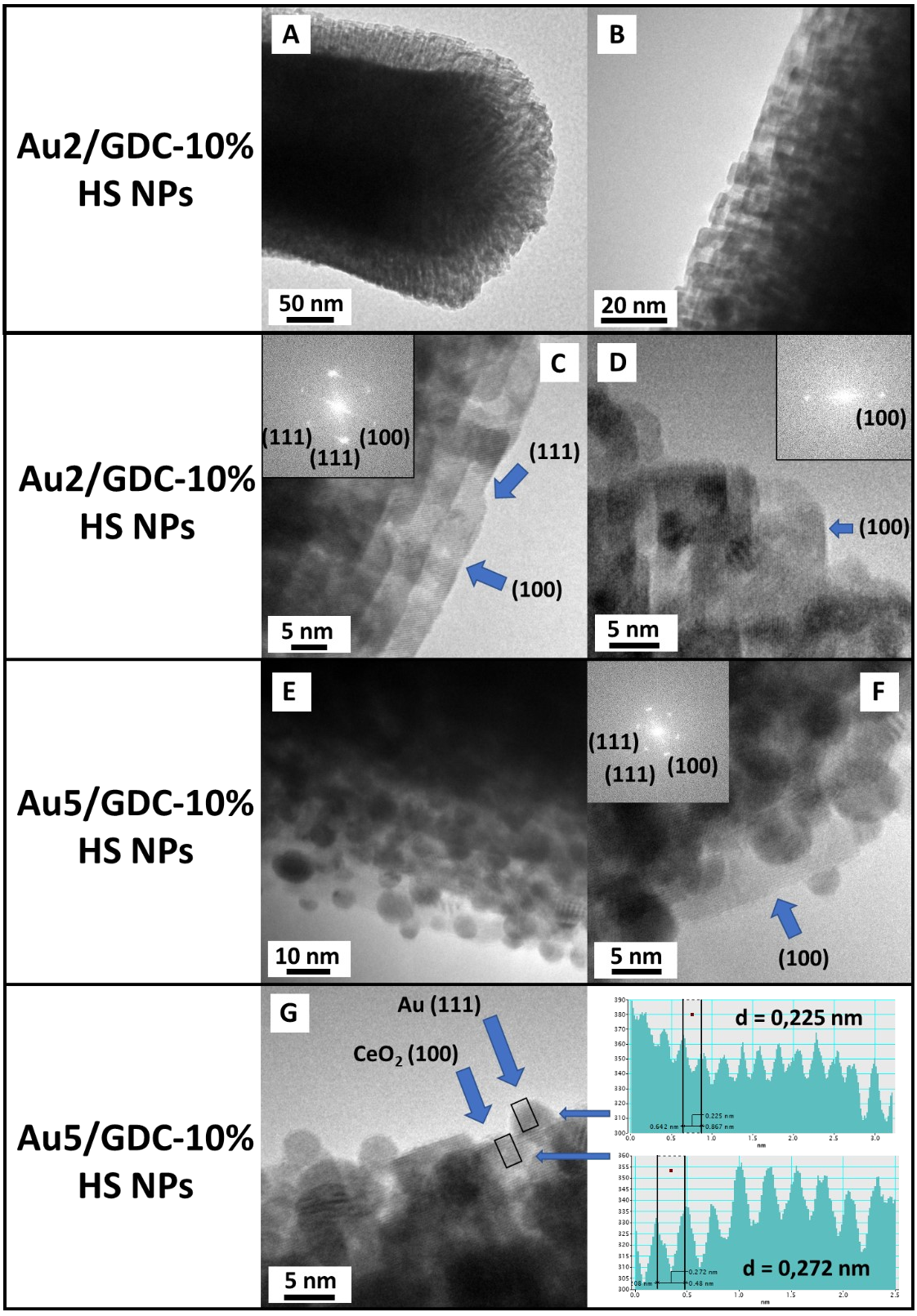

Fig. S6. Morphology of the external surface of the arms of star-shaped Au x/GDC-10% hierarchical catalyst (x denotes surface coverage parameter equal to 2 or 5). A-B) TEM images of Au2/GDC-10% arm showing plain support surface morphology; C-D) TEM images of Au2/CeO_2 showing dominant exposition of CeO_2(100) planes; E-F) TEM images of Au5/GDC-10% showing Au NPs embedded on CeO_2(100) planes; G-H) TEM images of Au5/GDC-10% showing Au NPs exposition of CeO_2(100) planes.

A)

Sample		TEM volume weighted mean	PXRD
NPs	CeO_2	8.0	7.7
	GDC-10%	6.0	6.1
Cubes	CeO_2	20.8	16.1
	GDC-10%	22.2	16.5
HS NPs	CeO_2	6,2	7.8
	GDC-10%	4.1	6.9

B)

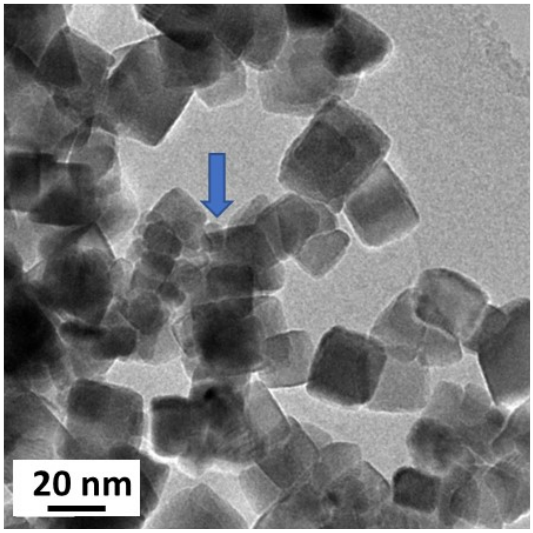

C)

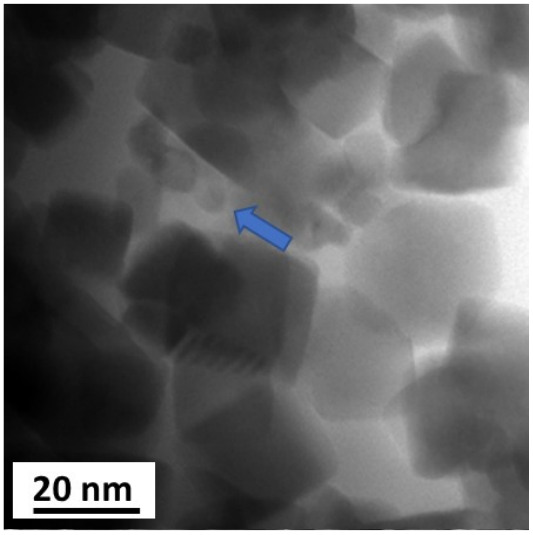

Fig S7.A. Volume-weighted mean size (obtained from TEM) vs mean size obtained from PXRD (Scherrer formula) of ceria particles differed by morphology; B) TEM image of CeO_2 cubes sample; small non-cubic (oval-shaped) crystallites marked by arrow , C) TEM image of GDC-10% cubes sample; small non-cubic (oval-shaped) crystallites marked by arrow.

A

Sample	Shapiro-Wilk test				Levene's test
	DF	statistic	p-value	Reject normality	
CeO_2 cubes	319	0,99048	0,03642	no	F(3,1237) = 25,27 p < .001
CeO_2 HSNPs	309	0,99348	0,20209	no	
GDC-10% cubes	324	0,99624	0,64081	no	
GDC-10% HSNPs	289	0,99476	0,42818	no	

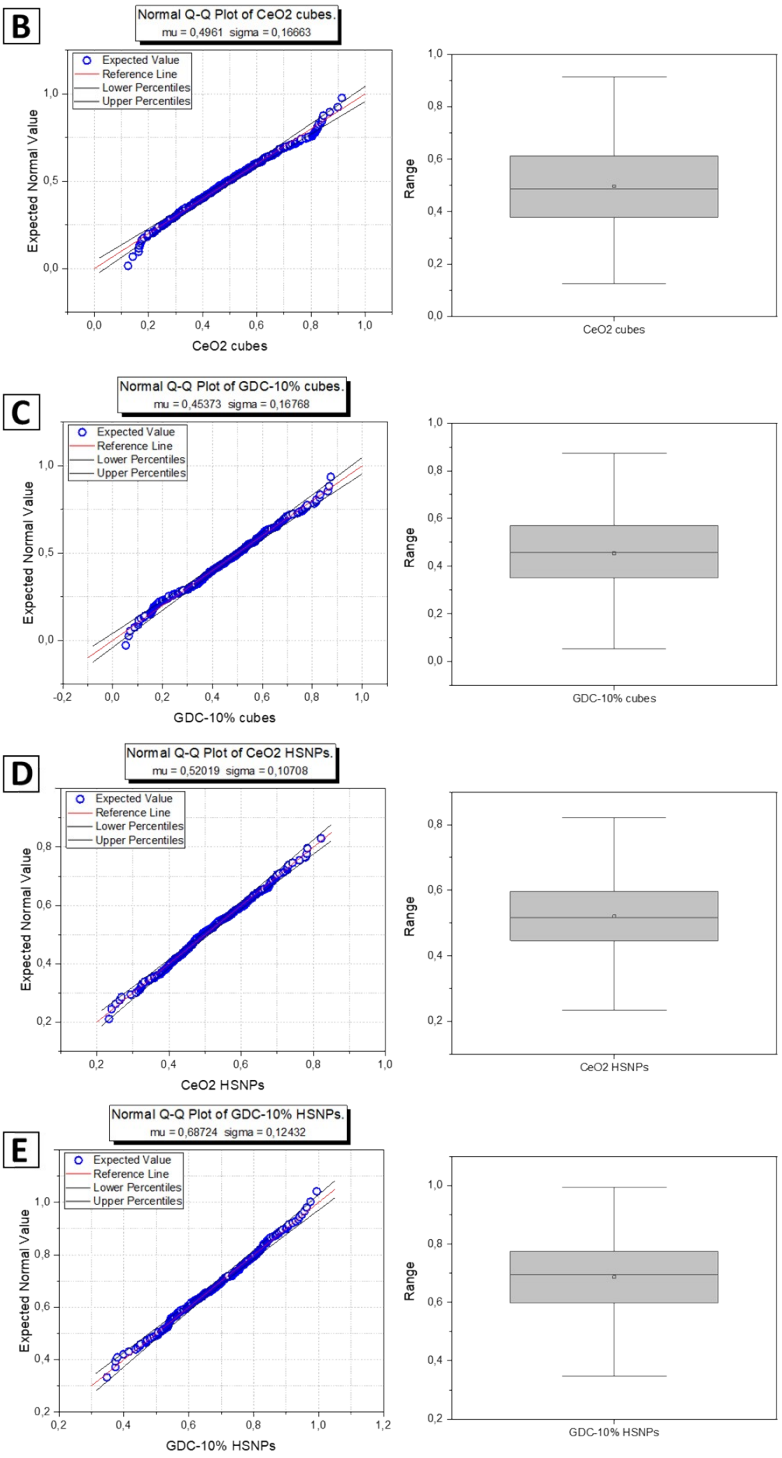

Fig. S8. A)) Shapiro-Wilk test and Levine's test results for AuNPs size data for supports differed by architecture and doping level. Samples are before propane oxidation (size data obtained from TEM); B-E) Q-Q plots and box charts for tested samples: B) Au5/CeO_2 cubes C) Au5/GDC-10% cubes D) Au5/CeO_2 HSNPs E) Au5/GDC-10% HSNPs. All samples are normally distributed. Variances are not

equal across groups, however, samples have similar size and outliers has been eliminated for statistical analysis of variance.

IR , TPD and iDPC-STEM results

Temperature programmed desorption (TPD) and infrared spectroscopy (IR) were conducted to investigate the surface chemical composition of hierarchical catalysts.

ATR-FTIR spectra do not show any dissimilarities between bare CeO_2 HSNPs support and its Au2 or Au5 gold-decorated counterparts (Fig. S9). All spectra show maxima characteristic to CeO_2 at 1550 cm^{-1} and 1391 cm^{-1} [1]. The maxima at 3400 cm^{-1} and 1638 cm^{-1} may be ascribed to water chemisorbed on the surface [2]. In line with this, increased H_2 release from hierarchically structured catalysts as compared to model cubic one is observed in CO-TPR experiment described in Section 3.2.2. As indicated in the literature, surface hydroxyls may play a significant role in stabilization and propagation of oxygen vacancies [3], the presence of which, in turn, is linked to facilitation of catalytic activity.

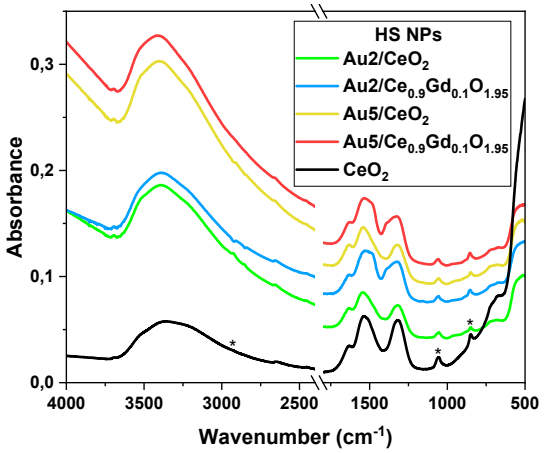

Fig. S9. ATR-FTIR spectra of the gold-decorated hierarchically structured catalysts. *Maxima corresponding to alcohol that was used during measurement.

TPD results for bare CeO_2 HSNPs show possible contamination of the sample with carbonaceous residues that form during thermal decomposition of cerium formate (Fig. S10). In particular, the desorption of CO_2 and CO above 400°C indicates presence of carbon contaminants not removed during calcination that has been conducted up to 400°C. In fact, acquisition of Integrated Differential Phase Contrast (iDPC) images in STEM mode, that has been taken in order to observe oxygen vacancies at the atomic level, was not successful due the high carbon contamination induced by electron beam interaction with the sample, at the present the process if contamination growth have been mainly attributed to adsorbed hydrocarbon molecules on the sample [4]. Presence of those carbon residues is presented in iDPC-STEM images (Fig. S11).

Simultaneous desorption of CO and H_2 at 750°C may indicate relatively strong adsorption of formate groups on CeO_2 surface. Stable carbonate moieties on the real catalyst surface have been observed by many authors [5][6]. As a prevailing view today CO_3 residues are thought to be spectator species in CO oxidation, although it was once thought that they took an active part in the reaction mechanism [7]. Also, Davó-Quiñonero et al. have shown that CeO_2(100) surface, which is the dominant surface in HSNPs studied in this research, have a strong tendency for binding of multidentate carbonates whose desorption is hampered [8]. Nevertheless, Chen et al. have observed

that the decomposition reactivity of carbonate species depends on size of AuNPs deposited on CeO_2 [9]. Trace NO amounts that coincide with CH_4 desorption may come from DMF that had been used as synthetic solvent. Also, the decent CO_2 maximum at 100°C indicates a large sorption capacity of the material, as this may be ascribed to CO_2 adsorbed from the air.

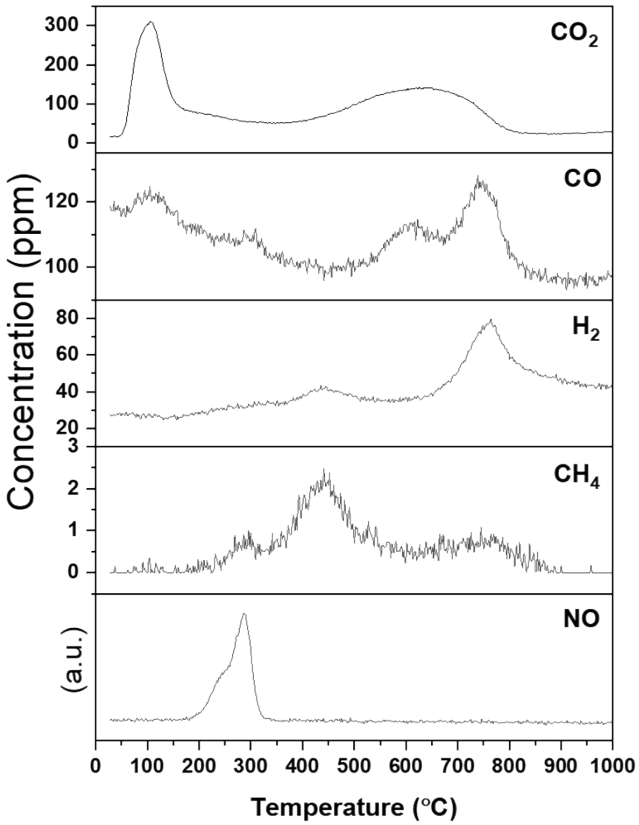

Fig. S10. The TPD curves obtained for bare CeO_2 hierarchically structured support (HSNPs).

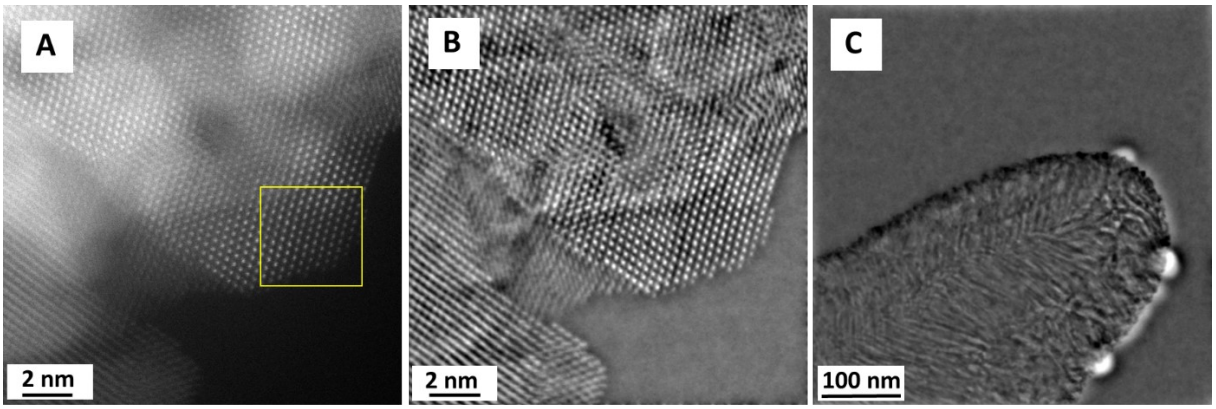

Fig. S11. HAADF images of GDC-10% carrier. A) High-magnification HAADF image; B) High-magnification iDPC-STEM image; C) Low-magnification iDPC-STEM image. iDPC technique is very sensitive to carbon contamination, as may be seen on low-magnification iDPC-STEM image. All zones analyzed were contaminated under image acquisition, therefore oxygen positions are not visible.

Literature

[1] P. Kumar, A. Kumar, C. Joshi, R. Singh, S. Saran and S. L. Jain, *RSC Advances*, 2015, **5**, 42414–42421.

[2] J. S. Lee and S. C. Choi, *Materials Letters*, 2004, **58**, 390–393.

[3] X. P. Wu and X. Q. Gong, *Physical Review Letters*, DOI:10.1103/PhysRevLett.116.086102.

[4] S. Hettler, M. Dries, P. Hermann, M. Obermair, D. Gerthsen and M. Malac, Micron, 2017, 96, 38–47.

[5] H. Liu, A. I. Kozlov, A. P. Kozlova, T. Shido, K. Asakura and Y. Iwasawa, J. Catal. 1999, vol. 185, 252-264.

[6] M. Maciejewski, P. Fabrizioli, J. D. Grunwaldt, O. S. Becker and A. Baiker, Physical Chemistry Chemical Physics, 2001, 3, 3846–3855.

[7] R. Meyer, C. Lemire, S. K. Shaikhutdinov and H.-J. Freund, Surface Chemistry of Catalysis by Gold, Gold Bulletin, 2004, 37, 72-124.

[8] A. Davó-Quiñonero, S. López-Rodríguez, C. Chaparro-Garnica, I. Martín-García, E. Bailón-García, D. Lozano-Castelló, A. Bueno-López and M. García-Melchor, Catalysts, 2021, 11(12), 1556.

[9] S. Chen, L. Luo, Z. Jiang and W. Huang, ACS Catalysis, 2015, 5, 1653–1662.

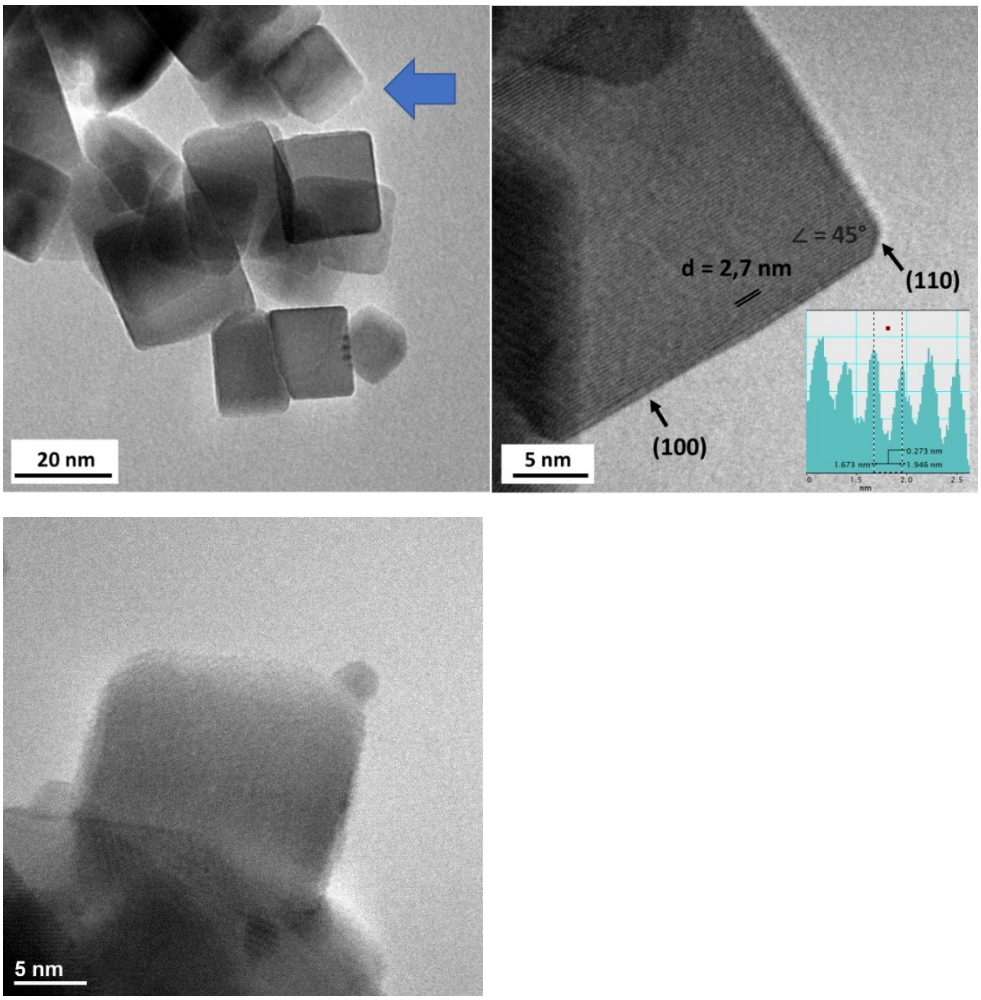

Fig. S12. TEM images of CeO_2 cubes. Deviation from regular cube morphology (egde- and corner-truncated crystallites); Au/5GDC-10% cubes (bottom image). Gold embedded on site deflected from cubic morphology.

A)

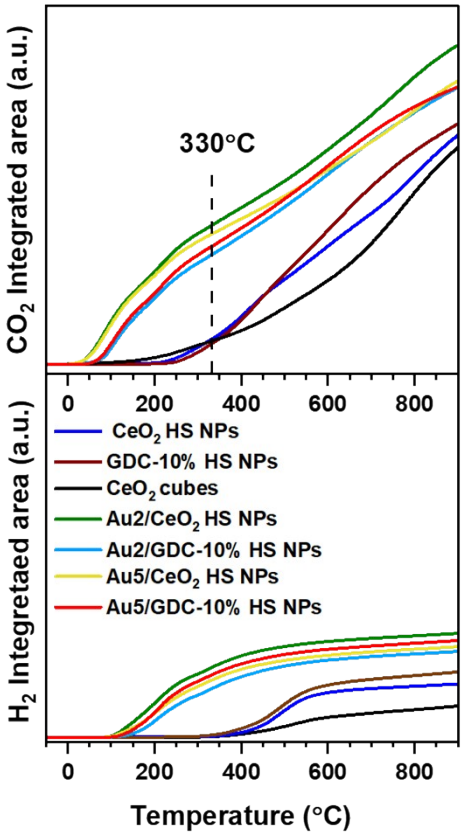

B)

Sample	Oxygen consumpation	
	surface (-25℃-500℃) (% total)	bulk (-500℃-900℃) (% total)
CeO_2 HS NPs	37	63
GDC-10% HS NPs	38	62
Au2/CeO_2 HS NPs	57	43
Au2/GDC-10% HS NPs	57	43
Au5/CeO_2 HS NPs	59	41
Au5/GDC-10% HS NPs	60	40

Fig. S13.A) Temperature dependences of the cumulative CO_2 and H_2 release during CO-TPR;
B) Surface vs bulk oxygen consumption calculated from CO-TPR data.

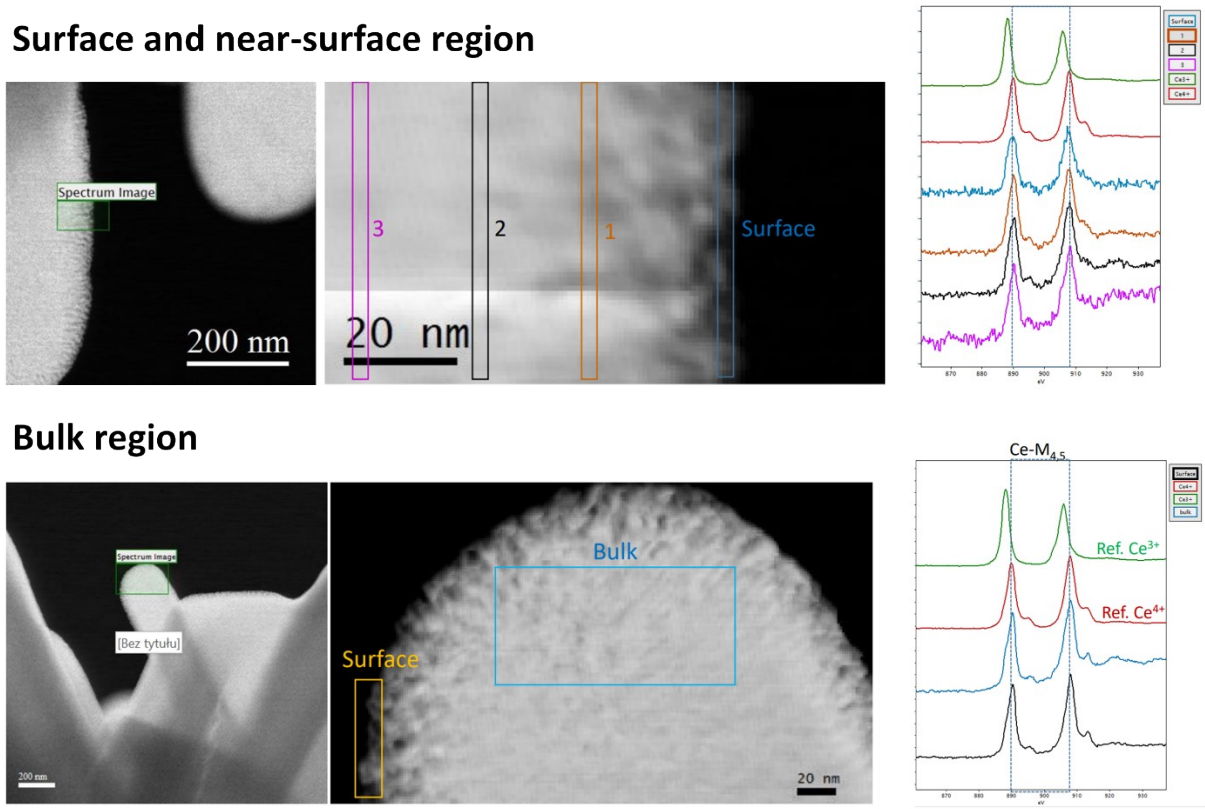

Fig. S14. EELS-SI analysis of the arm of star-shaped particle (CeO_2 HSNPs) in the surface/near-surface region (top), and bulk region (middle). Ceria reduction induced by electron beam has been also presented (bottom).

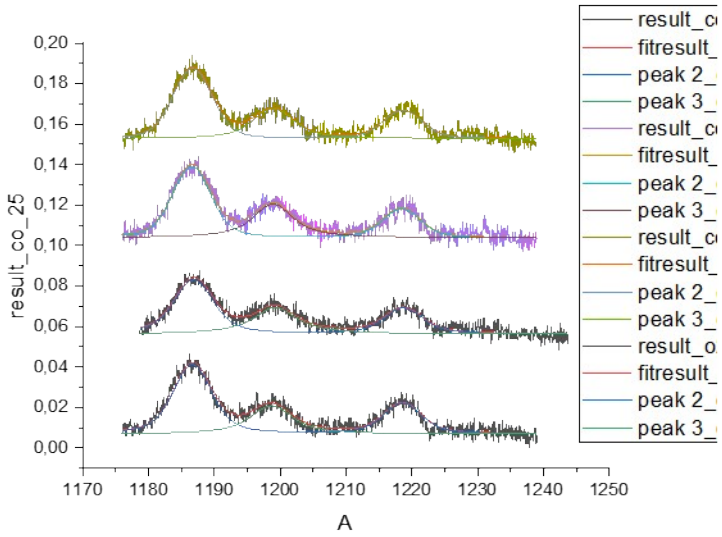

Sample	Ce3+/Ce	Au/Ce	Gd/Ce	Au+/Au
Au/CeO2@O2@573K	0	0.21	0	0.08
Au/CeO2@CO@300K	0	0.22	0	0.05
Au/CeO2@CO@373K	0.04	0.21	0	0.03
Au/CeO2@CO@473K	0.1	0.21	0	0.02
Au/GDC-10%@O2@573K	0	0.2	0.19	0.015
Au/GDC-10%@CO@300K	0	0.21	0.18	0.016
Au/GDC-10%@CO@373K	0	0.24	0.17	0.019
Au/GDC-10%@CO@473K	0.05	0.23	0.17	0.018

Fig S15. NAP-XPS of Au5/GDC-10% HS NPs (top); The relative abundance of Au ,Ce, Gd content and oxidation states in Au5/CeO_2 and Au5/GDC-10% determined using NAP-XPS (bottom). Relative contributions of the fitted components were calculated as the ratio of peak areas.

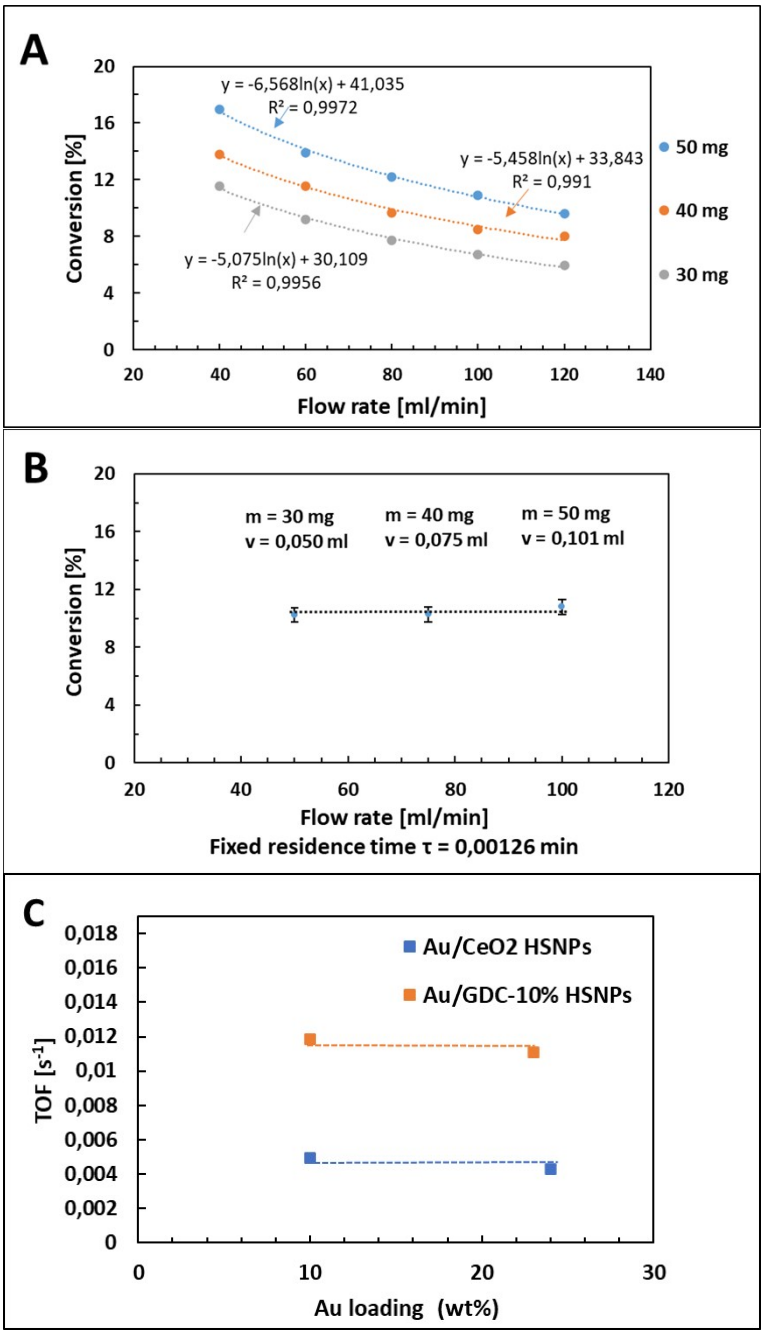

Fig. S16. Mass transfer limitation tests. A) Conversion as a function of flow rate for different loadings of CeO_2 HSNPs catalyst support in propane oxidation: 30mg, 40mg and 50mg. B) Diagnostic test for interphase transport limitation (Dautzenberg, 1989); plots of conversion versus flow rate in fixed residence time for different loadings of CeO_2 HSNPs support. C) The Koros-Nowak test ; plots of TOF versus Au loading at 25℃ for Au/CeO_2 HSNPs and Au/GDC-10% HSNPs.

F. M. Dautzenberg, Ten guidelines for catalyst testing , Characterization and Catalyst Development, Chapter 11, ACS Symposium Series, Vol. 411, 1989, pp. 99–119.

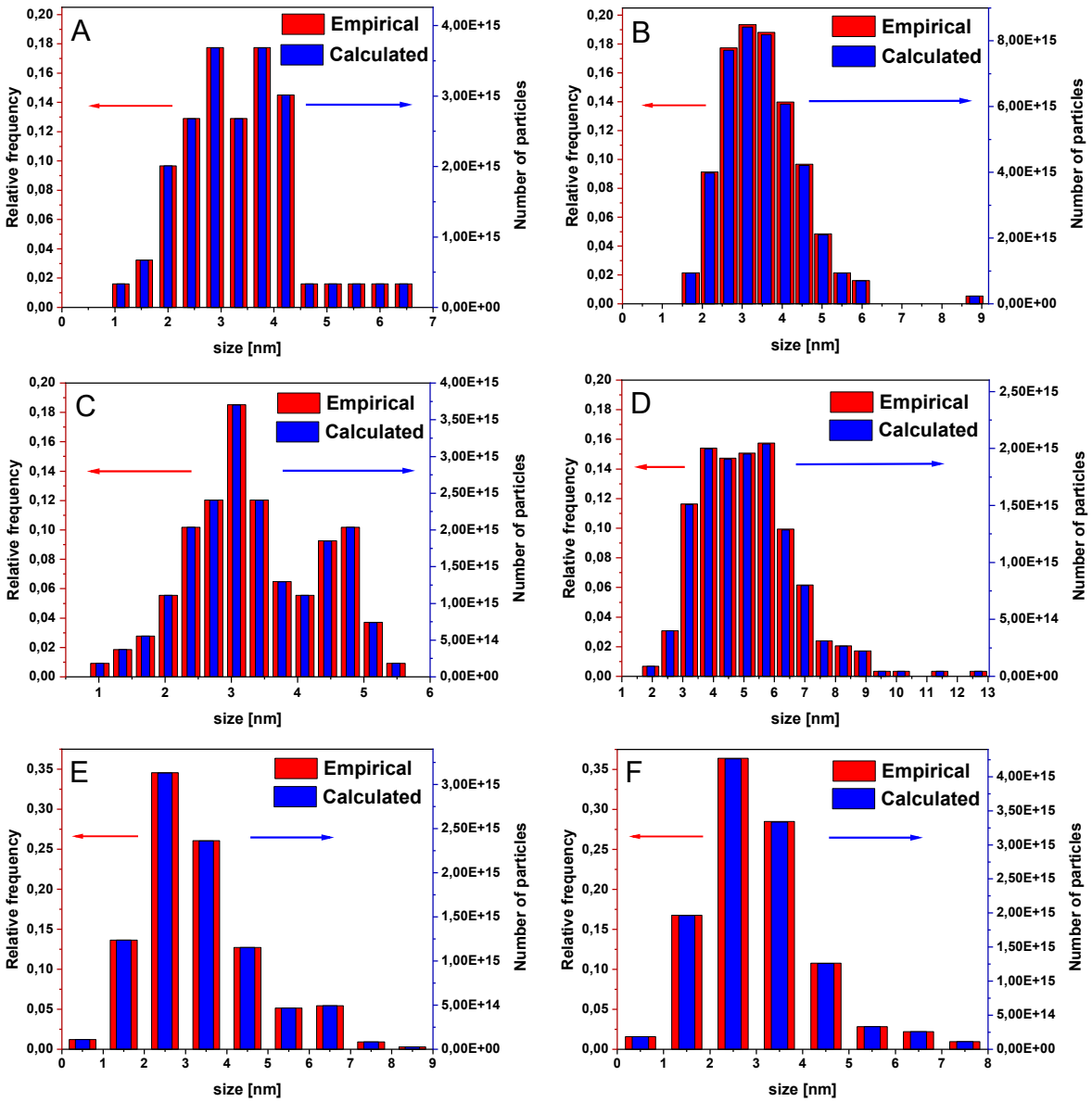

Fig. S17. Histograms showing empirical Au NPs size distribution determined from TEM (lefts axis) and corresponding number of Au particles (modeled as half-spheres) calculated via the use of Solver tool with restriction to total mass of active phase (Au-wt%) in 0,05g catalyst (right axis). A) Au2/CeO_2 HSNPs; B) Au5/CeO_2 HSNPs; C) Au2/GDC-10% HSNPs; D) Au5/GDC-10% HSNPs; E) Au5/CeO_2 cubes; F) Au5/GDC-10% cubes.

$TOF_{[b]}$ calculation

$TOF_{[b]}$ defined as specific rate normalized to the number of active sites at the Au/ceria interface (ring around Au nanoparticle, Au NP modeled as a half-sphere) has been calculated from the following formula: $TOF_{300°C}$ [s^{-1}] = $r_{300°C}$ [mole of propane·g^{-1}·s^{-1}]/(mole of Au/ceria interface active sites [mole]/mass of the Au active phase [g]). The mole number of Au active sites at the Au/CeO_2 interface was determined from empirical histograms generated from TEM data. Firstly, Solver tool in Excel was used to determine number of particles that corresponds to empirical histograms (Fig. S13.2 A-F). The total volume that corresponds to the mass of the active phase in 0,05g catalyst has been chosen as objective cell, while relative frequency as constraints to model the total number of the Au half-

sphere nanoparticles redistributed to each bin of the histogram. The number of Au interface atoms that correspond to each size interval of the histogram has been calculated from the number of Au particles in a bin, the diameter of the Au NP and van-der-Waals radii of Au atom (166 pm).

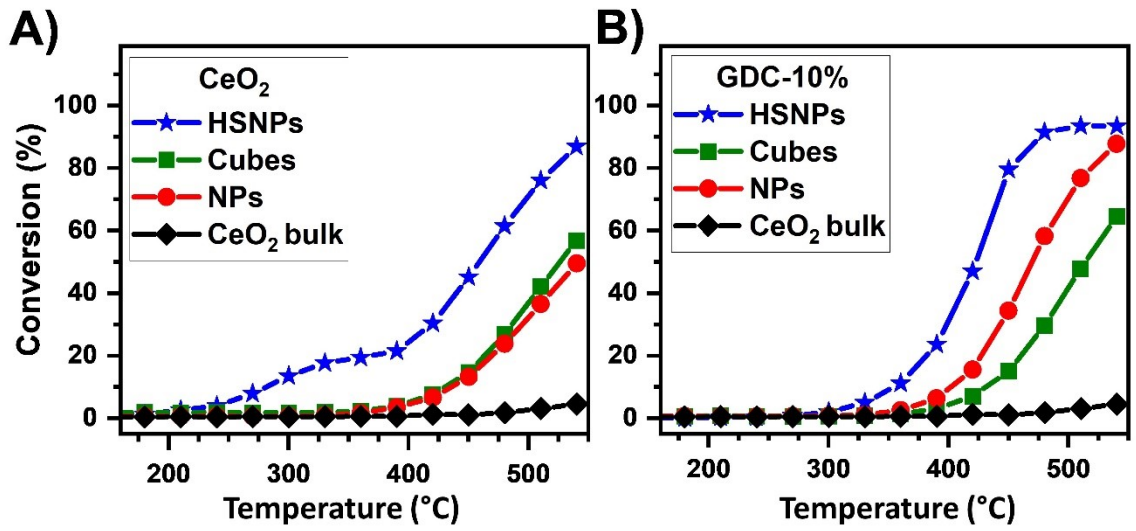

Catalyst support	r X 10^6 [mol $m^{-2} h^{-1}$]	
	330℃	420
CeO_2 NPs	1,4	10,8
CeO_2 cubes	8,0	32,2
CeO_2 HSNPs	15,1	25,9
GDC-10% NPs	1,2	17,9
GDC-10% cubes	3,4	27,9
GDC-10% HSNPs	3,8	36,5

Fig. S18. Propane conversion plots of samples differing by support morphology, nanoparticles (NPs), nanocubes (cubes), hierarchically structured particles (HSNPs); A) CeO2 supports, B) GDC-10% supports; C) specific rate at 330℃ and 420℃.

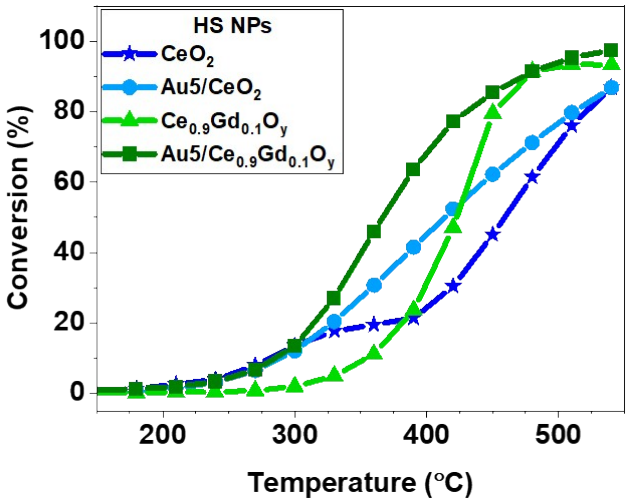

Fig. S19. Propane conversion of $Ce_{0.9}Gd_{0.1}O_{1.95}$ (x=0;0.1) HS NPs carrier and Au5/ $Ce_{0.9}Gd_{0.1}O_{1.95}$ (x=0;0.1) HS NPs catalyst.

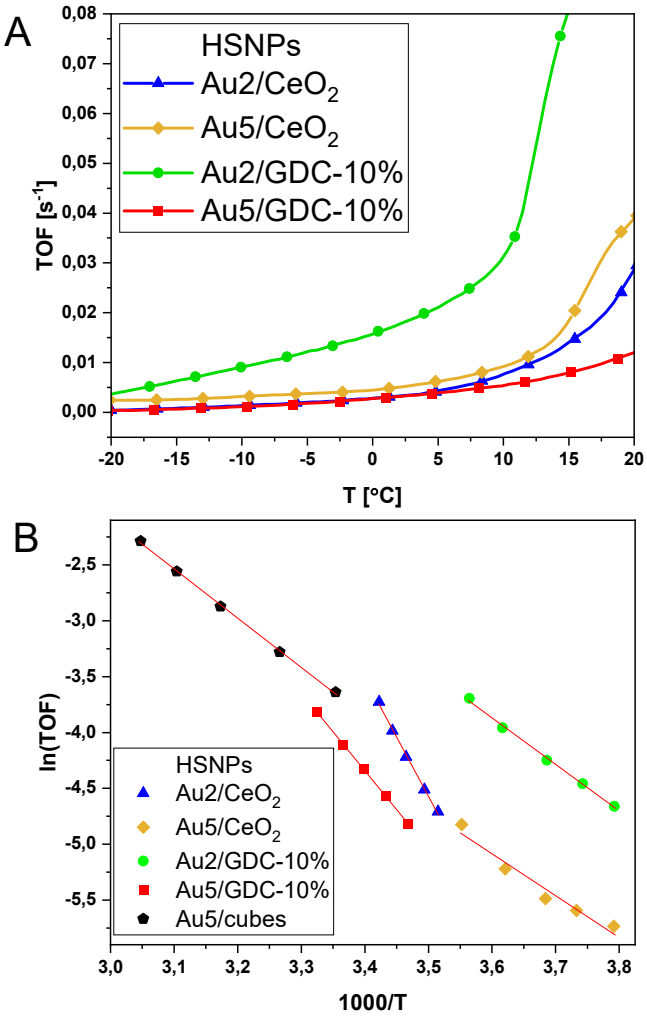

Fig. S20. Catalytic performance in CO oxidation. A) TOF as a function of temperature; B) corresponding Arrhenius plots.

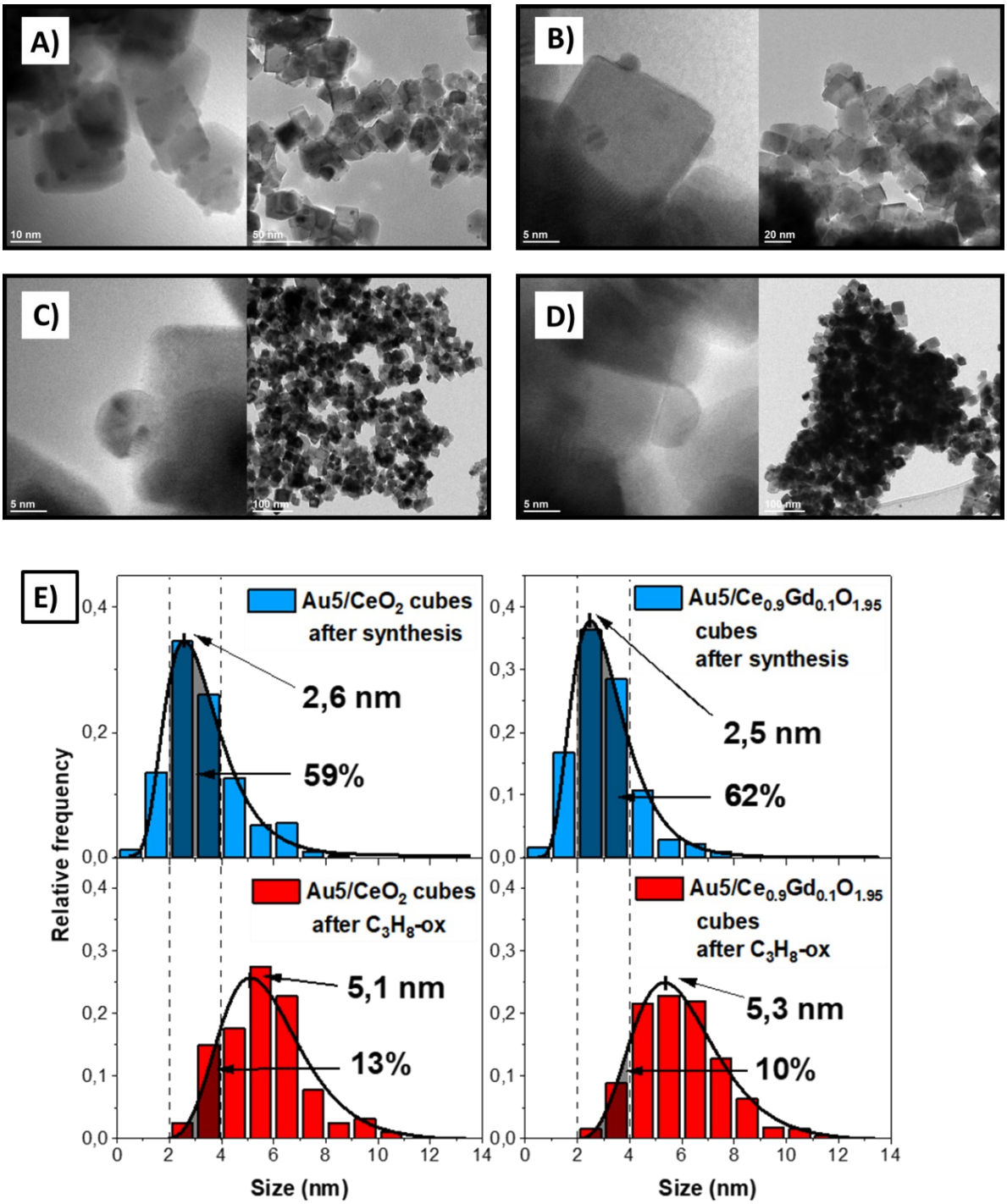

Fig. S21. TEM images of $Ce_{1-x}Gd_xO_{2-x/2}$ (x=0; 0.1) cubes before and after propane oxidation. A) Au5/CeO_2 cubes before oxidation; B) Au5/GDC-10% before oxidation; C) Au5/CeO_2 cubes after oxidation; D) Au5/GDC-10% after oxidation; E) Au NPs size distribution plots.

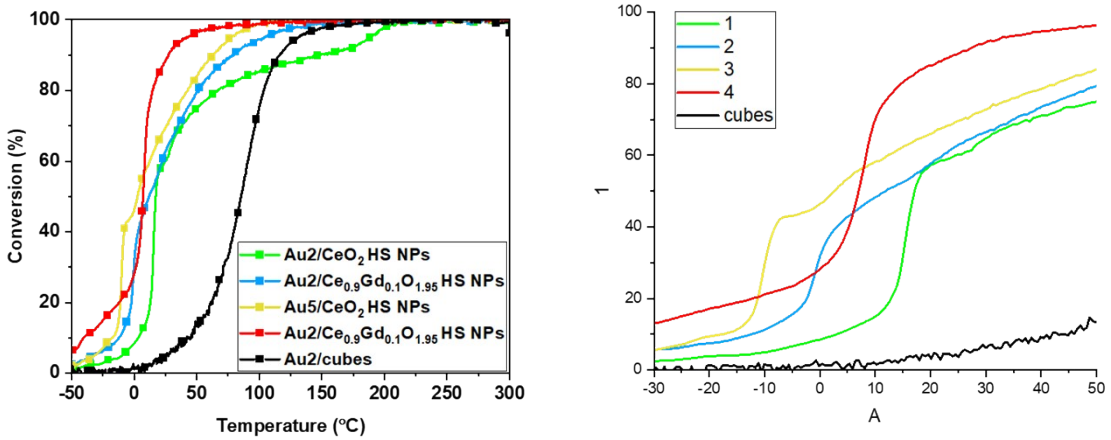

Fig. S22. CO conversion plot of hierarchically structured catalysts after reduction in H_2 flow at 400℃ for 3h.

A

Sample	Shapiro-Wilk test				Levene's test
	DF	statistic	p-value	Reject normality	
CeO_2 cubes	325	0,99373	0,19779	no	F(3,1307)= 14,92627 p < .001
CeO_2 HSNPs	325	0,99641	0,67782	no	
GDC-10% cubes	335	0,99349	0,15775	no	
GDC-10% HSNPs	326	0,99333	0,15814	no	

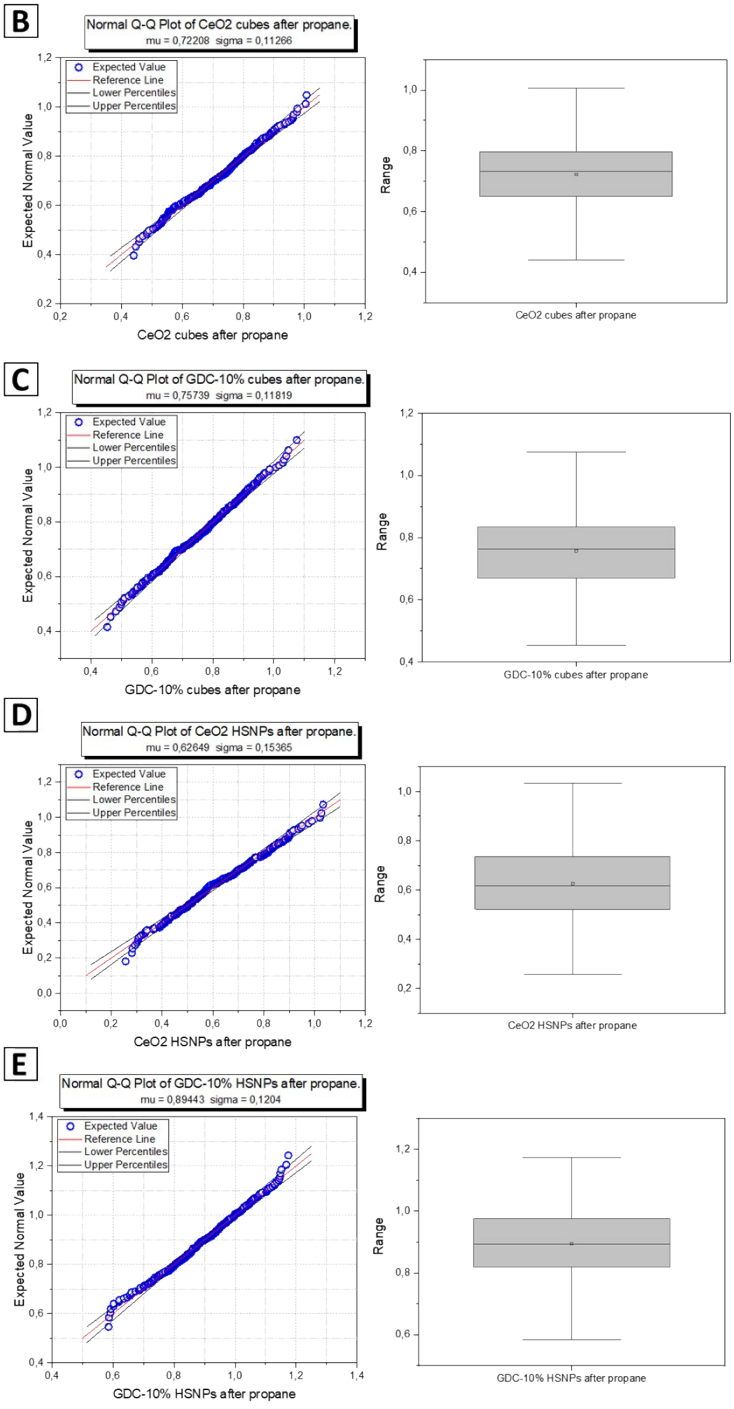

S23. A) Shapiro-Wilk test and Levine's test results for AuNPs size data for supports differed by architecture and doping level. Samples are after propane oxidation (size data obtained from TEM); B-E) Q-Q plots and box charts for tested samples: B) Au5/CeO_2 cubes C) Au5/GDC-10% cubes D) Au5/CeO_2 HSNPs E) GDC-10% HSNPs. All samples are normally distributed. Variances are not equal across groups, however, samples have similar size and outliers has been eliminated for statistical analysis of variance.